



PERGAMON

Organic Geochemistry 33 (2002) 613–634

**Organic  
Geochemistry**

www.elsevier.com/locate/orggeochem

# Equations of state in exploration

Peter Meulbroek

*Materials and Process Simulation Center, California Institute of Technology, Chemistry 139-74, Pasadena, CA 91125, USA*

## Abstract

Calculations using equations of state to predict the phase behavior and composition of hydrocarbon species are finding use as an exploration technique. Equations of state give insight into the chemical changes induced in a hydrocarbon mixture by changes in pressure and temperature. Equation of state calculations can be used to estimate the effects of alteration during migration, reservoir filling, and production. Production effects explored include reservoir depressurization and pumping-induced fractionation. Other reservoir management techniques discussed include volume prediction, fluid fingerprinting, and oil quality estimations. Migration effects addressed include gas washing and evaporative fractionation. © 2002 Published by Elsevier Science Ltd.

## 1. Introduction

Equations of state have been used for many years in production-related simulations to estimate the GOR and density of reservoir fluids. Though these production-type numbers are of interest to the geochemist, of more interest would be the change in quantities currently measured by the geochemist, such as biomarkers or fingerprinting compounds. For geochemists to have impact on solving production problems, the traditional equations of state must be modified to accept compounds more familiar to the geochemist. In principle, a traditional equation of state can automatically incorporate (e.g.) extended hopanes or steranes. In practice, such incorporation is fraught with difficulty, since interactions between species of interest and the bulk fluid can be non-ideal. This work describes some of the extensions necessary to make equations of state a useful exploration and geochemical analysis tool, and gives some examples of the use of this tool.

The traditional role of Equations of State within the petroleum community has been within the realm of resource exploitation. A study of fluid phase behavior is a standard part of the development of hydrocarbon fields. Most fields will have PVT analyses performed on one or more reservoir sands so that reservoir engineers can predict the response of the fluids to production. A

PVT analysis produces a description of that fluid as a combination of real, measured compositions and a series of pseudo-components—lumps of undifferentiated components defined by a boiling point cut in the case of distillation, or carbon number in the case of a pseudo-distillation using a gas chromatograph. An equation of state is typically used to perform PVT calculations that supplement and extend the measurements from the PVT analysis. The goal of these calculations is to provide accurate density and GOR predictions of the reservoir fluid throughout production. Although very complex expressions can be used to predict the density and phase behavior of reservoir fluids, most practitioners chose either a complex empirical relationship (such as the BWR equation of state, with 9 adjustable parameters) or, more commonly, a cubic equation of state.

Equations of state have been used by the chemical and chemical engineering communities since Guy-Lussac, Boyles, Charles, and Avagadro each formulated their gas-phase relationships between the intrinsic state variables (pressure, temperature, intrinsic volume, and molar amount). These relationships are combined in the ideal gas law. At the end of the 19th century, the ideal gas law was modified by van der Waals (1873) to account for additional forces between gas particles. His basic assumption—that the forces between gaseous particles are linear and separable into attractive and repulsive forces—still underlies present-day equation of state work. Many of the equations of state used currently—Redlich–Kwong–Soave, Peng–Robinson, et cetera—rely on this assumption.

*E-mail address:* meulbroek@wag.caltech.edu

Though used in reservoir management, equations of state have not found widespread acceptance in the exploration community. However, it has long been recognized that certain phase-behavior questions are important in exploration. Sokolov et al. (1963) published work on oil migration in a compressed gas or water solution, which implies a fractionation process of some sort. That same year, Silverman (1963) and Silverman and Plumley (1963) first described the process of separation-migration. This process involves a phase separation caused by changes in pressure and temperature, followed by migration of the two phases along separate paths. Silverman conceived that these pressure and temperature changes arise from either migration or tectonic forces.

In the 1970s, as geochemists questioned the method by which petroleum migrated, Price (1976) suggested that petroleum migrates as an aqueous solution. This led to a rebuttal by McAuliffe (1979), who argued that the process of dissolving into water and then separating from water would fractionate oil, and leave a fluid very unlike that found in petroleum reservoirs. Eventually, a consensus was reached that hydrocarbons migrate as a separate phase, and the ideas of phase fractionation fell into disuse.

In the late 1980s, Thompson (1987) recognized that many of the gas condensates in the Gulf of Mexico basin resulted from phase fractionation. He proposed that in situations where enough methane mixes with single-phase oil to cause phase separation, the result is a gas condensate and a residual oil. Thompson's concepts were supported by Larter and Mills (1991), who performed experiments to determine the compositional changes that a migrating fluid undergoes. The Larter and Mills experiment simulated the migration of methane charged oil from a higher pressure and temperature regime to a lower one. During the simulated migration, the experimental fluid underwent a phase separation. Larter and Mills sampled both phases of the fluids, directly measuring the chemical effects of phase separation. Later experimental work includes that by Van Graas that more precisely measures fractionation patterns under a series of fractionation scenarios.

There is evidence in the literature that phase fractionation occurs in many areas around the world. Fluid compositions that appear to result from phase fractionation occur in the US Gulf Coast (Thompson, 1987) offshore Taiwan (Dzou and Hughes, 1993), the Norton Basin, Alaska (Kvenvolden and Claypool, 1980), the South China sea (Zhang and Zhang, 1991), and the Mahakam delta, Indonesia (Vandenbroucke and Durand, 1983). Of these sites, the clearest examples of phase fractionation are found in the US Gulf Coast, the Mahakam Delta, and offshore Taiwan. Thus, the types of problems that can be addressed by equations of state have worldwide application.

Some numeric work has been published using equations of state to address exploration or geochemical uses (Sylta, 1991; Wendebourg, 2000), and more work has been presented at conferences. Several of the commercial basins modeling packages include equation of state-driven compositional models. The models are focused on accurately predicting volumes of fluid, and have yet, in the authors experience, to achieve the compositional resolution necessary to capture the behavior of compounds of interest to the geochemical community. That being said, some cross-over work has relied successfully on these models. For example, di Primio et al. (1998, 2002) have used an equation of state to model the phase behavior of mixtures, using the shapes of the calculated phase envelope as a fingerprinting technique.

For the organic geochemist, equations of state represent a new and exciting potential. The combination of the detailed chemical analysis techniques available to the organic geochemist and the predictive abilities of the equation of state have the potential to revolutionize the role of the organic geochemist within the exploration and development communities. There are two areas of applications of equations of state of interest to the exploration or production geochemist. In production activities, equations of state can predict changes in composition due to fluid phase equilibration at changing ( $P$ ,  $T$ ) conditions caused by reservoir production. A carefully designed model can predict both changes in bulk properties, such as GOR or API gravity, and changes in compounds of geochemical interest, such as biomarkers, within both the migration conduit and the reservoir. Within the reservoir, equations of state can be used to predict the relationship between the composition of the fluid coming up the drill pipe and the conditions within the reservoir and thus calibrating 'geobarometers', and distinguishing the processes that affect reservoir fluids. In exploration activities, equations of state can be combined with basin modeling and maturation modeling to predict phase behavior and composition of migrating fluids. The knowledge gained can be used as a calibration for basin modeling, as a risk-management input (e.g. a prediction of the quality of known deeper liquids), or used directly as an exploration device by making predictions about the existence of untapped resources.

This work will explore the form of common equations of state, with particular emphasis on the Aasberg-Petersen equation of state (Aasberg-Petersen and Stenby, 1991). All the equations used will be cubic—that is, relate pressure to the cube of specific volume—in the van der Waals separable form. The equations used in this work include that by van der Waals, the Mathias equation of state (Mathias, 1983), the Predictive RKS (Holderbaum and Gmehling, 1991), as well as the Aasberg-Petersen and Stenby (A-PS) equation of state. It will then address several extensions of equations of state

to petroleum fluids using pseudo-components to model complex mixtures, interaction parameters, and liquid-vapor equilibrium. Finally, the work will address equations of state modeling in geology and geochemistry, both in reservoir applications and in exploration applications.

## 2. Modeling subsurface fluids

There are several differences between modeling of migrating fluids and modeling of entrapped fluids. The first difference lies in initial constraints, such as the fluid flux rates through the system. The second difference lies in boundary conditions, such as the flow in and out the system by fluids of differing maturities.

In traditional equation of state modeling, a reservoir is treated as a closed system with a fixed composition. Though this is clearly a simplifying assumption (since a producing reservoir is open to the drill pipe), the high rate of production compared to the rate of equilibration means that this assumption is usually reasonable. Thus, any changes in composition due to, e.g. disequilibrium production, do not propagate throughout the reservoir over the timescale of production. For example, in a two-phase reservoir the act of lowering the reservoir's pressure during production will tend to change the composition within each phase present within the reservoir, since the composition of each phase is a function of ( $P$ ,  $T$ ,  $z$ ) conditions. In the absence of active transport phenomena, the main equilibrating mechanism within a reservoir is molecular diffusion, and order-of-magnitude rates of fractionation and re-equilibration can be estimated. England (1990) finds that vertical equilibration rates are on the order of  $10^5$ – $10^6$  years, while lateral equilibration rates are on the order of  $10^6$ – $10^7$  years. For a typical reservoir, this gives diffusion fluxes of mm/year. These rates are much slower than production, where fluxes on the order of meters per day near the well bore are common, implying that the vast majority of reservoir fluids maintain the same chemical composition throughout the production process except near a phase boundary (the gas cap, the oil-water contact, or the production well-bore). However, pressure-induced gas cap formation (where the system goes from one to two phases) should lead to bulk compositional changes, since these effects permeate the reservoir due to the density differences between exsolved gas and the parent oil.

Within the migration conduit, however, the much slower flow rates, large surface areas of contact between phases, and small volumes imply that chemical equilibrium between phases is much more likely here than in the reservoir. Since the migrating fluid is subjected to much larger changes in ( $P$ ,  $T$ ) conditions than the reservoir fluid, phase separations within the conduit

must be taken into account when modeling fluid composition. Hence, computation of chemical changes due to pressure and temperature changes must use a more sophisticated model than would be needed to model closed-systems such as reservoirs.

The second difference between modeling a reservoir and a migration conduit is that mixing with allochthonous fluids occurs more frequently for migrating fluids than for reservoir fluids. The high surface area to volume ratio of a migrating fluid allows equilibrium interaction with other fluids occur more easily for a migrating fluid. Furthermore, focused flow through migration conduits such as faults tends to increase the chance of interaction between different fluids. It is necessary, therefore, that the equations of state models applied to migration are designed to handle open systems with radically changing composition.

## 3. Equation development

To understand the impact of equations of state on exploration in general and geochemistry in particular, a brief history and derivation of an equation of state are presented.

Two types of models are generally lumped together under the moniker of 'equation of state'. To solve the composition problem, a fluid phase equilibria model determines the number and composition of phases that minimizes the Gibbs free energy of a fluid; i.e. when the fugacities of all the components of the system are constant across all phases of the system. Hence, a fluid phase equilibria model requires values for the fugacity of each component of the system in each phase. An equation of state in the most abstract form relates the following intensive properties of a fluid: pressure, temperature, density, and composition. In most common form, the equation expresses either pressure or density as a function of the other intensive variables. Fugacity is a 'corrected' partial pressure of a component, and represents the sum of deviations from ideality of that component. An equation of state can be used calculate these deviations, and so can be integrated to predict the fugacity of each component of a system. The combination of the two models can be used to predict the complete state of a complex multi-component fluid system, and to predict the changes in that system with changing state variables.

The first equations of state related two state variables in ideal gases.<sup>1</sup> Boyles's Law predicts a linear relationship between pressure and density. Charles Law predicts a linear relationship between temperature and volume. Avagadro's hypothesis relates the volume and number

<sup>1</sup> An ideal gas is a fluid composed of point-like particles that only interact by elastic collisions.

of particles in a system. The Ideal Gas Law combines these relationships to relate pressure, volume, amount, and temperature. This equation is valid for ideal gas-phase fluids approaching the limits of infinite temperature, infinite volume, and zero pressure.

The Ideal Gas Law was modified by van der Waals to accommodate real-world fluids by relaxing the two assumptions of an ideal gas. In the van der Waals model, molecules are considered to be hard-shell spheres of finite, non-zero volume,  $b$ .<sup>2</sup> The molecules interact with attractive forces that decay with the square of distance, characterized by the attraction parameter,  $a$ . The two forces sum linearly, giving an equation in the following form:

$$\left(P + \frac{a}{v^2}\right)(v - b) = RT. \quad (1)$$

To date, the van der Waals-type cubic equation of state remains the most common form for equations of state. The equations are referred to as cubic because they are cubic in volume when put in polynomial form. This type of equation has two terms: a 'repulsive' term and an 'attraction' term. The 'repulsive' term takes into account the volume occupied by individual molecules of the fluid. The 'attraction' term takes into account all attractive forces between the molecules of a fluid, including ionic, coulomb, and hydrogen bonding. Since a cubic equation can have multiple roots, cubic equations of state can predict several possible values for volume at a given pressure and temperature; in particular, cubic equations of state can predict both the liquid and the vapor phase volume of a fluid.

The general form for a cubic equation of state is as follows:

$$P = \frac{RT}{v - b} - \frac{a(T)}{v^2 + c_1v + c_2}. \quad (2)$$

Different equations are defined by using different values for  $c_1$  and  $c_2$ . The attraction parameter,  $a$ , is always a function of temperature and composition, while  $b$  is often considered to be a temperature-independent function of composition.

### 3.1. The Redlich–Kwong equation of state

One of the earliest cubic equations of state was developed by Redlich and Kwong (1949). Redlich and Kwong modified the original van der Waals form by letting  $c_1 = 1$  and  $c_2 = 0$  in Eq. (2), and thus defined a cubic equation of state of the following form:

$$P = \frac{RT}{v - b} - \frac{a}{v(v + b)}. \quad (3)$$

Both  $a$  and  $b$  are determined from theoretical assumptions.<sup>3</sup>

Though accurate for many mixtures, the Redlich–Kwong equation of state does not work well for mixtures that contain large molecules or incompressible gases (species that have low critical temperatures). In particular, the Redlich–Kwong equation of state produces inaccurate results for mixtures of long-chain (e.g. *n*-alkane) hydrocarbons. This was remedied in the early 1970's as Soave (1972) modified the mixing rules for ' $a$ ', above.

The resultant Redlich–Kwong–Soave (RKS) equation has seen widespread acceptance as a method for calculating fluid properties. There have been many schemes (see Reid et al, 1985) presented to modify the RKS equation since Soave's original paper in 1972, including Michaelsen (1990), Lielmezs and Mak (1992), Tsonopoulos and Heidman (1986). These schemes usually modify the mixture attraction parameter  $a$ . The modifications do not generally improve the overall accuracy of equations of state beyond the general mixing rules proposed by Soave (Shibata and Sandler, 1989). Instead, the equations tend to be tuned for different regions of ( $P$ ,  $T$ ) space. In general, the RKS equation of state is adequate for non-polar mixtures if pressure and temperature conditions are far from the mixture's critical point. A note of caution about these numbers: the cubic EOS generally over-predict liquid molar volume (i.e. under-predict density) (Chou and Prausnitz 1989).

Other equations of state, such as the A-PS (Aasberg-Petersen and Stenby, 1991) or Behar EOS (Behar et al., 1985), that move away from the traditional Redlich–Kwong format can improve on predictions of, e.g. fluid density. Recent developments include the incorporation of results from excess Gibbs Free Energy models (such as UNIFAC or UNIQUAC) to estimate the  $k_{ij}$  parameters. To demonstrate the accuracy of the various models, a comparison between the intrinsic volume predictions for methane of several equations of state is shown in Fig. 1.

Fig. 1 shows the percentage error in the predictions by several equations of state for methane molar volume at 350 °K. Shown are four different equations of state: the original van der Waals equation of state, the Predictive Redlich–Kwong–Soave, the A-PS, and the Mathias (1983). For this particular test, the A-PS

<sup>3</sup> The equation assumes that the first and second partial derivatives of state variables are zero at the critical point, as proposed by van der Waals to assure the continuity of the liquid and vapor states.

<sup>2</sup> Corresponding to van der Waals radii.

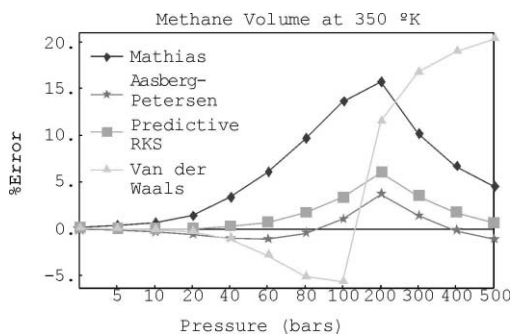


Fig. 1. Comparison between different equations of state. Shown here are the van der Waals, Predictive Redlich–Kwong Soave (PRKS), Aasberg–Petersen (A–P), and Mathias (an RKS-type EOS).

EOS clearly does the best job of matching experimental volume predictions over the entire range of pressures. We will use this equation of state in all later examples.

Note that more details for this estimation can be found at <http://www.wag.caltech.edu/home/meulbroek/EOS>, including source code for the models used to make the estimation.

#### 4. Fluid phase equilibria

Equations of state predict the relationship between pressure, temperature, and volume for real-world fluids, including fluid mixtures. They do not predict the phase behavior of fluids mixtures. Although equations of state can have multiple volume roots, these multiple roots have physical meaning only for single species fluids. For mixtures, the equation of state might have a single root, yet the mixture might actually divide into two or more separate phases. In order to determine the number and composition of phases into which a mixture will separate, a fluid phase equilibria (FPE) model must be used. The basis behind an FPE model is that any fluid system will seek the number and composition of phases that minimize the Gibbs free energy of the system. The system described here will estimate vapor–liquid equilibrium. It is certainly possible, and in some cases desirable, to predict multi- (> 2) phase equilibrium. For the petroleum system, there are undoubtedly 4–5 phases present somewhere in the migration conduit between source rock and reservoir. Beyond liquid and vapor, there is water ubiquitously present and at least in local equilibrium, asphaltenes are commonly thought to form a solid phase colloid within the petroleum, and solid kerogen forms a phase within source rock. There are some ( $P$ ,  $T$ ) conditions where an excess of  $\text{CO}_2$  might form a separate,  $\text{CO}_2$ -rich liquid phase. There are

chemical reactions between, e.g.  $n$ -alkanes in oil and alkanolic acids dissolved in water. These acids might interact with inorganic phases such as calcium carbonate, changing their equilibrium distribution. Hence, a full petroleum chemical system is very complex, indeed. The major fractionation mechanism, however, is probably petroleum liquid–vapor, since the solubility of hydrocarbons is highest in these phases. Hence, for simplicity’s sake we restrict our explorations to two-phase systems.

The fugacity coefficient of a component in a fluid represents the sum of all deviations from ideality of that species. For an equation of state that is pressure explicit (where molar volume is calculated as a function of pressure), the ideal condition is zero pressure; i.e. a completely diffuse gas. These deviations are summed as the mixture is brought from ideal conditions to the conditions of interest. The unknown values in this equation are  $V$  and  $\partial P/\partial n_i$  (see Appendix). Hence, to calculate the fugacity coefficient requires a model that can calculate both the volume and the derivative of pressure with respect to composition for a mixture over arbitrary temperatures and pressures.

Several different types of models exist that can provide these values. Though an equation of state can be used, there exist specialized functions for each of the potential phases that may provide more accurate estimates of fugacity in that phase than the generic EOS estimate. The choice depends on the ( $P$ ,  $T$ ) conditions and the composition of the system. For a vapor phase, an equation of state can provide adequate accuracy over any pressure and temperature range. For the liquid phase, an equation of state is often used at high pressures, or for simple mixtures, such as mixtures of hydrocarbons (Lin and Daubert, 1978). An equation of state for both liquid and vapor-phase fugacities is an accepted method for high-pressure (pressure greater than 10 bars) conditions (Reid et al., 1985). Using an equation of state in both the liquid and vapor phases is preferable if the equation of state can provide sufficiently accurate results, since this insures continuous values for fugacity.

For more complex mixtures (such as mixtures including water), at certain ( $P$ ,  $T$ ) conditions, several immiscible liquid phases can form. In this case, an equation of state might not provide sufficiently accurate results. The problems are twofold. First, as stated previously, equations of state do not accurately predict the volumes of complex mixtures, though specialized equations of state exist (Shock and Helgeson, 1990). Secondly, the integration starts at a reference state of infinite volume (zero pressure). At this reference state, the phase in question might not exist, and so calculating its properties might not be possible. Instead, a different reference state must be the starting point for the integration.

#### 4.1. Binary mixing parameter

All values used in the equations of state within this manuscript can be calculated or obtained from published tables, with the exception of the interaction parameter,  $k_{ij}$ . This parameter is a ‘fudge factor’ that lumps complex non-ideal interactions between molecules into a single factor. The parameter is used to adjust model output to fit either vapor pressure or PVT data. Knowing precise values for  $k_{ij}$  is important for either high precision volume calculations or for mixtures that contain very dissimilar species. For pure hydrocarbon mixtures, precise values for  $k_{ij}$  are not essential (i.e. all  $k_{ij}$  values for these mixtures are close to 1) (Soave, 1972).

For hydrocarbon–hydrocarbon interactions, parameter estimation is provided in Pedersen et al. (1984), which gives interaction parameters as a function of molecular weight:

$$k_{ij} = 1 - 0.00145 \frac{MW_i}{MW_j} \quad (4)$$

For mixtures containing non-hydrocarbons or lumped components, accurate values for  $k_{ij}$  parameters are vital for predictions of phase behavior. In particular, an unbiased cubic equation of state does a poor job at predicting the behavior of mixtures containing polar species. An example helps emphasize this point. A mixture of a polar, associating species and a polar solvent, such as water, tends to deviate from ideality. These deviations can be addressed using appropriate  $k_{ij}$  values. Even mixtures that are not handled well by equations of state, such as mixtures containing a species that tends to dimerize, can be adequately modeled.

To demonstrate this point, a binary mixture of formic acid (HCOOH) and water at STP is flashed at different concentrations, and the specific gravity predicted. In this example, the formic acid molecules are mostly dimerized. Without tuning, an equation of state cannot predict accurate mixture bulk properties. This point is made by Fig. 2, which plots the density of a mixture of formic acid and water as a function of concentration. This figure clearly shows that the A-PS equation of state, with its extra terms, best fits the experimental data, though “best” is a clearly relative term, since the maximum errors are on the order of 20%. All other equations of state tend to under predict density for this mixture by a factor of two or more. Note that this implementation of the A-PS equation of state includes the Wang and Gmehling (1999) correction, which uniformly increases density predictions using a scalar correction.

Fig. 3 shows experimental density data compared to predictions calculated using the A-PS equation of state at a variety of temperatures over a range of concentrations. The predictions set all  $k_{ij}$  values to unity. Note that the predictions are poor, and get increasingly bad

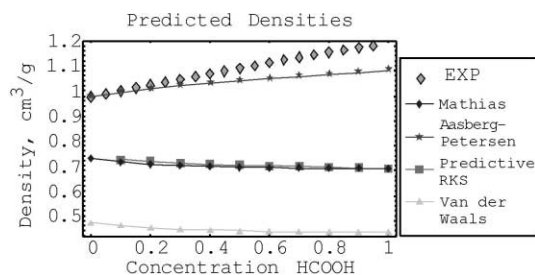


Fig. 2. Predicted densities of a mixture of formic acid (HCOOH) and water, as a function of mole fraction acid. Exp is the measured density. All other labels are defined above.

with increasing concentration of formic acid and increased temperature. However, by utilizing an adjustable parameter in Eq. (8), the modeled system gets much closer to the experimental, as shown in Fig. 4.

Fig. 4 shows the experimental versus modeled density for water at a variety of temperatures over the full range of concentrations. By utilizing an empirical parameter (adjusted here to minimize the RMS error between predicted and experimental values), the model does a much better job of predicting the solution density. We can continue to improve the accuracy of predictions with increasing numbers of adjustable parameters, but the marginal gain in accuracy decreases with increasing interaction parameters. The most important interaction factor is between HCOOH and HCOOH, where the interaction parameter doubles the attraction term.

It must be noted that theoretical methods for estimating interaction parameters have been developed in recent years. These methods (Vidal and Lermite, 1979; Holderbaum and Gmehling, 1991; Dahl and Michelsen, 1991) rely on the UNIFAC model, a group-contribution chemical activity model, to predict the interaction between species. The power of UNIFAC is that interactions between species are estimated by adding contributions from functional groups in each species. This means that interactions can be estimated for species without using direct experimental data. These methods are ‘semi-empirical’ since the interaction between functional groups is estimated by utilizing a training set of binary 2-phase equilibria data (Fredenslund et al., 1977). Though details of this model are beyond the scope of this manuscript, code the algorithms are instanced in the “Hydrocarbon Toolkit”, an open source *Mathematica*-based set of routines to calculate phase equilibrium available for download at <http://www.wag.caltech.edu/home/meulbroek>.

#### 5. Pseudo-components

If the compositions of migrating organic phases were known accurately, application of the above model

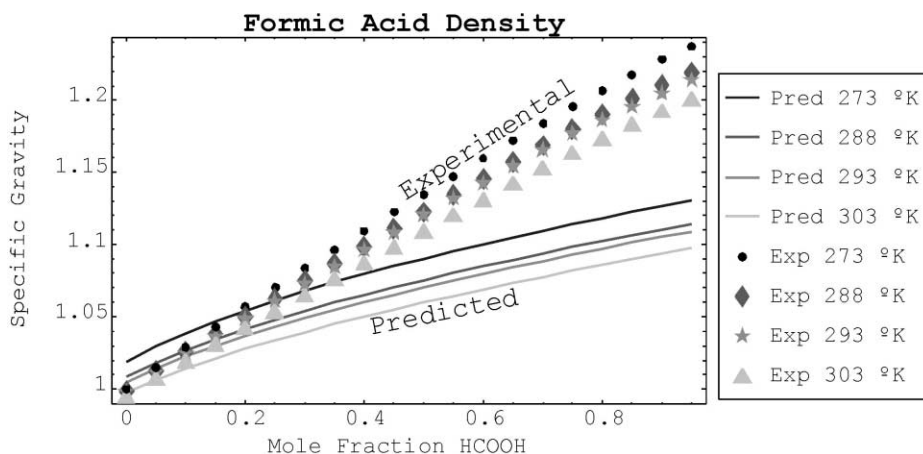


Fig. 3. Predicted versus actual density for formic acid solution. The predicted densities are calculated using the A-PS equation of state with no  $k_{ij}$  adjustments.

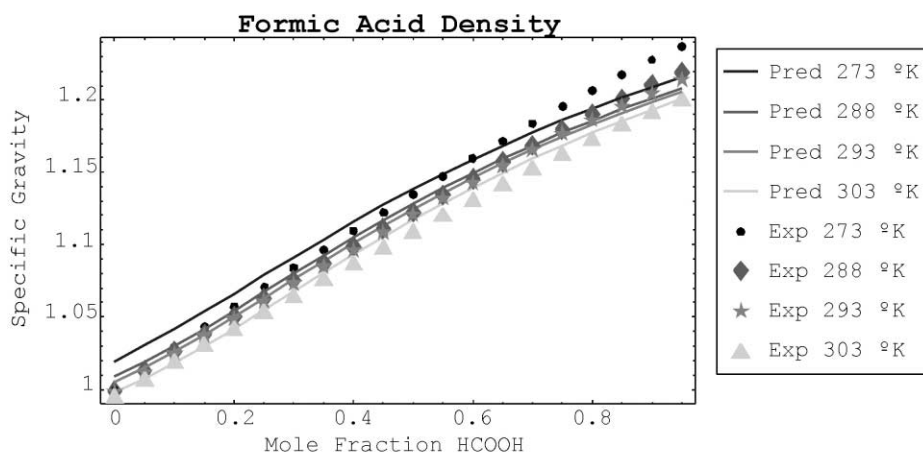


Fig. 4. Predicted versus actual density for formic acid solution. The predicted densities are calculated using the A-PS equation of state with a single  $k_{ij}$  adjustment to HCOOH–HCOOH interactions.

would be straightforward. Binary interaction parameters could be measured experimentally or estimated computationally. The phase behavior of the mixture could be predicted using the models described herein and calibrated using binary mixing data. Unfortunately, two issues add complexity to the modeling of subsurface fluids. The composition of the fluids emerging from source rock is not well constrained, except in very special cases where the source rock is the reservoir rock, since it is subject to change throughout the migration process. Secondly, the tremendous diversity of organic compounds in the organic phase results in a computationally challenging problem. Estimates for the number of components in oil range from  $10^6$  to  $10^8$ . The solution to these dilemmas proposed for reservoir modeling is to use lumped components, where the lumping scheme is

defined by a separation technique. Lumping ignores the chemical diversity, and smoothes out some of the chemical changes due to mixing.

Two common lumping schemes group components based on boiling point (as defined by distillation), or on GC retention time (as defined by pseudo-distillation). Both these schemes group compounds by something akin to volatility. The boiling point lumping, now largely superseded for PVT analysis, uses a distillation process to separate the mixture into a number of boiling point fractions. This process suffers the limitation that one compound might occur in several lumps. For example, the boiling point of *n*-decane is 345 °F, and so it is present in appreciable quantities in the first three distillation cuts (Altgelt and Boduszynski, 1994). The second scheme, known as pseudo-distillation, uses either

GC or a GC/SCFC combination to divide species into carbon-number lumps. Though molecular isomorphism also affects retention time, the scheme is a large improvement compared to distillation.

These schemes define pseudo-compositions that can be used by equations of state to accurately estimate fluid bulk properties for closed systems (such as a virgin reservoir) or systems whose compositional rate-of-change is much greater than the rate of equilibration (such as a producing reservoir). These schemes DO NOT WORK WELL in systems where the compositional rate-of-change is near the equilibration rate, such as in the migration conduit. The problem in these settings is that changes in composition can result in ‘property drift’ where the real composition of pseudo-components can change over time. ‘Property drift’ is an example of a fractionation process, where a lump (e.g. the C10 components) can have different compositions in the liquid and vapor phases. The underlying components that make up that lump will separate unequally into the two phases. In order to minimize property drift, the pseudo-component scheme has to be modified to take the volatility of the species contained within the pseudo-component into account. This can be accomplished by sub-dividing carbon-number lumps into sub-lumps defined by chemical family (Pendersen et al., 1989). Several schemes have been developed to subdivide these lumps (so called ‘splitting schemes’), also based on separation techniques, such as SARA and PIN. These splitting schemes go beyond the scope of the current work, and form an area of active research.

## 6. Applications

### 6.1. Method

In the following section, several simulations are presented to illustrate the utility of equations of state and fluid phase equilibria models in petroleum exploration. These examples explore changes in geochemistry during production, and changes in oil chemistry during migration. Though the geochemist has been focused on studying field data to understand what oil chemistry might infer about subsurface processes (either production or migration), equations of state give the geochemist tools to predict the chemical effects of likely scenarios, and provide pointers in understanding subsurface processes “from the perspective” of the fluid.

The specific model used has been ported and improved within the context of a *Mathematica* application, and released as open source under the GNU “CopyLeft” license at <http://www.wag.caltech.edu/home/meulbroek> as the “Hydrocarbon Toolkit”. The released code consists of a two-phase flash model based on several different equations of state that handles mixtures of arbitrary

complexity including pseudo-components. A number of other modules, including critical property estimations and several mixing rules, are included. The reader is urged to download the software and play with it him/herself, and is welcome to modify it for any purposes allowed under the CopyLeft agreement. The calculations shown here are typical examples of what can be done with equations of state. Further details of all calculations can be found at <http://www.wag.caltech.edu/home/meulbroek/>.

### 6.2. Traditional

#### 6.2.1. Volume predictions

The most common application of equations of state in petroleum science is in predictions of volume for reservoir fluids. Typically, the geochemist is not as interested in this application, unless it is predictive rather than descriptive. Some possible predictive applications of equations of state include the volume of material evolving from the source rock (Braun and Burnham, 1990; Meulbroek, 1997) and change-of-volume during migration or phase fractionation events. The following will present several calculations using equations of state. To explore a few of the uses of traditional EOS in reservoirs, a pseudo-composition has been assembled in Table 1. This pseudo-composition is taken from an average of several PVT reports from an area in the US gulf coast, and is intended only as an example. Note that, in all equation of state modeling calculations that follow, the ‘Cx’ components are modeled as *n*-alkanes of the same carbon number. This is a strong assumption, but not uncommon. It is made for ease of calculation; neither the numeric model nor the equation of state algorithm demands that components are ‘real’. Thus, the calculations presented here are most appropriate for waxy, paraffinitic crudes.

In exploration, determining the GOR of untapped fluids can strongly impact the economics of resource development, as can oil quality. Hence, estimations of fluid properties as a function of depth can be a useful risk-management tool. As an example of this type of calculation, consider the simple mixture of hydrocarbons specified by Table in a ‘typical’ sedimentary basin with conditions similar to areas in the Gulf of Mexico. The basin is overpressured beyond 2 km depth, with a 25 °C/km temperature gradient, hydrostatic pressure gradient above 2 km, and lithostatic gradient below 2 km. Since we are only interested in the change of a property with respect to changes in (*P*, *T*) conditions, this can be simulated with a series of flash calculations.

Data are developed by taking the initial mixture and flashing it at a series of pressures and temperatures determined by the (*P*, *T*) gradients defined above. The flash model then predicts liquid composition, vapor composition, and vapor fraction (the amount of



Table 1  
Pseudo-components of typical US Gulf Coast reservoir fluid

Component	Mol%	MW	Component	Mol%	MW
Nitrogen	3.74	28.013	C13	0.176	175
Carbon dioxide	3.457	44.01	C14	0.118	190
Methane	58.838	16.043	C15	0.083	206
Ethane	11.6	30.07	C16	0.057	222
Propane	5.957	44.097	C17	0.042	237
iso-Butane	1.701	58.123	C18	0.03	251
<i>n</i> -Butane	2.603	58.123	C19	0.022	263
iso-Pentane	1.399	72.15	C20	0.015	275
<i>n</i> -Pentane	1.417	72.15	C21	0.011	291
C6	1.189	84.	C22	0.007	305
Benzene	0.242	78.12	C23	0.005	318
C7	2.701	96.	C24	0.004	331
Toluene	0.412	92.15	C25	0.003	345
C8	1.608	107	C26	0.002	359
C9	1.195	121	C27	0.002	374
C10	0.704	134	C28	0.001	388
C11	0.412	147	C29	0.001	402
C12	0.244	161	C30+	0.002	550

material, by mole, in the vapor phase). Given two-phase composition, it is a straightforward inversion of the equation of state to predict its specific volume (volume/mole), and a simple calculation to determine its density. If the petroleum migrates from a source rock at 7 km (expulsion temperature: 190 °C) its density changes during migration as predicted by the A-PS equation of state are shown in Fig. 5. In Fig. 5, the liquid, vapor, and average mixture density (in g/cm<sup>3</sup>) are plotted as a function of depth. The fluid is within the two-phase regime above two km, leading to differences in density between the phases. Below 2 km depth, only one phase is present. Note also that, in the two-phase region, density tends to decrease in the liquid phase and increase in the vapor phase. This counter-intuitive decrease in density in the liquid phase is related to the amount of gas dissolved in the liquid; i.e. liquid GOR. Gas solubility

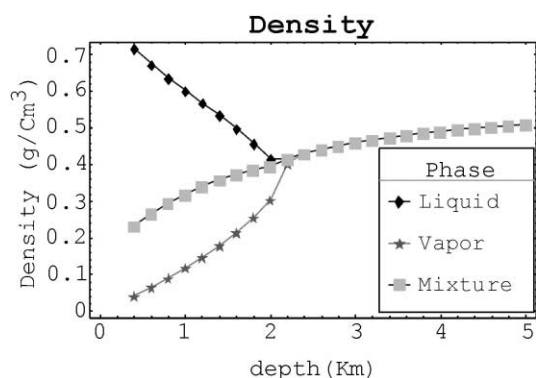


Fig. 5. Change in density with change in depth for a 'typical' oil.

increases with depth. This point is confirmed in Fig. 6, which plots the GOR of the liquid phase (i.e. the amount of gas dissolved in the liquid) as a function of depth. Only the two-phase region is plotted (since the GOR is constant for the entire one-phase region). GOR is estimated by taking the liquid composition, flashing it at STP, and calculating the volume ratios of the two resultant phases.

The difficulty of predictive volume calculations is the uncertainty in compositional models available to the exploration geochemist. Typically, compositional information on migrating petroleum either comes from analogy to reservoir fluids or predictions from a maturation model. Both approaches are fraught with difficulty. The analogy method fails in areas with complex migration histories, where the relationship between any reservoir fluid and the migrating fluid is subject to interpretation

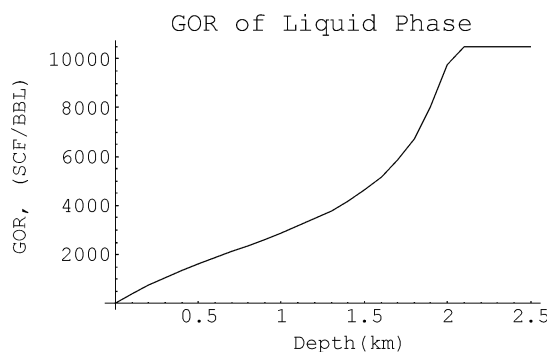


Fig. 6. GOR of the liquid phase in the above example, as a function of depth (hydrostatic pressure, 25 °C/km).

of such things as mixing ratios and original fluid maturity. In fields with multiple sources, the composition of any parent fluid (and hence, the prediction of the parent's density as a function of pressure and temperature) is uncertain without further constraints. Furthermore, mixing phenomena such as gas or water washing can change the bulk properties of the fluid without strongly affecting the composition of the heavy components; i.e. without leaving unambiguous evidence in some cases. Hence, the use of reservoir fluids as analogy to migrating fluids requires additional constraints in complex cases.

Using a maturation model to determine migrating fluid composition adds an additional layer of uncertainty to the above problem. The typical maturation model describes a hydrocarbon fluid using between 2 and 10 pseudo-components. As described above, pseudo-components are appropriate for describing mixtures in closed systems, such as reservoirs over non-geological time scales. In open systems, the pseudo-component problem tends to decrease the effectiveness of the models.

The applications of equations of state to this type of mixture rely on first estimating the critical properties of the pseudo-components, and then tuning the model appropriately to replicate any phase information available. Typically, a composition for a reservoir fluid is derived from a "PVT report" on the fluid, which will include a pseudo-distillation composition such as is shown in Table as well as a P-V chart which can be used for EOS tuning. Only a few tuning parameters are needed to move EOS predictions close (in a least-squares sense) to the measured data, as demonstrated previously. This method is acceptable when a sample of the fluid is available for experimental PVT measurements. In the application of equations of state to migration, such fluids are not typically available, and so the ability of a pseudo-component scheme to accurately predict bulk properties needs to be examined.

An important consideration in designing a pseudo-component scheme is how complex the mixture need be to accurately simulate the desired characteristics of the simulation. 'Black Oil' models, where the 'mixture' consists of 1 oil and 1 gas component are still prevalent in the literature and in commercial packages. On the other end of the spectrum, we have performed simulations using mixtures of several hundred compounds. The more complex mixtures tend to consume large amounts of computer power and take a long time to complete. More complex mixtures are not suitable, then, for embedding in larger-scale, higher dimension models (such as reservoir or basin simulators), while simple models might not be suitable for understanding compositional shifts due to large-scale processes.

Why, then, use a more detailed model? The lumped model above is reasonable at predicting bulk properties

of fluids under very strict closed system conditions. If the exploration geologist, modeler, or organic geochemist is interested in considering other estimations, such as molecules of geochemical interest, or at simulating open systems, the closed-system model breaks down, as will be shown in the next example.

#### 6.2.2. Reservoir management applications

Equations of state have typically been used to predict bulk fluid properties in reservoirs, such as GOR and density. Of more interest to geochemists is the ability of equations of state to predict chemical changes during production, and hence to be useful in reservoir management schemes. The composition of produced reservoir fluids changes over the lifetime of the reservoir. There are several reasons for this change. These include pressure-induced gas-cap fractionation, where declining reservoir pressures force the more-volatile species out of solution and into the gas cap, and production fractionation, where producing a single phase (e.g. an oil leg) removes relatively more of the less-volatile species in a multiphase reservoir fluid, altering the overall composition. The differences between these two scenarios are important. Declining pressures in a reservoir does not necessarily mean that it is being actively produced; it may be in pressure, but not compositional, communication with a producing reservoir. A producing reservoir should show compositional shifts that reflect production fractionation. If these two scenarios can be differentiated, it can have important implications in production allocation and reservoir delineation. This type of modeling is only valid in the two-phase region, where strong density differences can drive mixing. The scenario is simplified to emphasize the utility of equations of state. A more realistic model would utilize an equation of state embedded within a reservoir simulator. Such an idea is not new, as existing reservoir simulations typically rely on flash calculations. The importance of the work shown here is that calculations added compositional detail can reveal more information about processes within the reservoir.

In this example, two scenarios are compared: the first when a reservoir is in pressure (but not fluid) communication with a producing reservoir, and so is depressurized without fluid loss, and the second when a two-phase reservoir is produced for liquid (but not for gas). In the later case, compositional differences between the vapor and liquid phases will result in fractionation of the mixture composition.

In the first scenario, a decrease in pressure tends to cause an increase in the size of the gas cap, as gas comes out of solution. The scenario places the oil defined above in Table 1 at a depth of 1.8km, where the mixture is at its bubble point. Over time, this mixture is subjected to decreased pressure at a constant temperature, simulated by repeated isothermal flash calculations at

lower and lower pressures. For the drawdown scenario, a mixture is flashed at a series of pressures ranging from 180 bar down to 10 bar, at 55 °C. The flash calculation gives the vapor fraction (fraction of the mixture in the vapor phase, by mole) as well as composition of the liquid and vapor phases.

Decreasing the pressure tends to increase the amount of material in the vapor phase, as shown by Fig. 7. Fig. 7 shows the vapor fraction of the mixture defined in Table 1 as a function of reservoir pressure (constant temperature). The vapor fraction is defined as moles vapor per mole mixture. It is a useful modeling number since it overcomes weaknesses of other indicators of the size of the vapor phase: it is immune to the pressure and temperature dependencies from which volume indicators suffer, and is not affected from normalization issues that mole fraction estimates suffer.

As a comparison, Fig. 8 shows the change in gas cap size (as defined by volume ratio in standard cubic feet/barrel) with changing pressure during a drawdown scenario. Note the increasing curvature on the left-hand side of the curve. At shallow depths (low pressure), the density of the gas phase drops quickly, resulting in very large gas caps. Hence, GOR is a better representation of

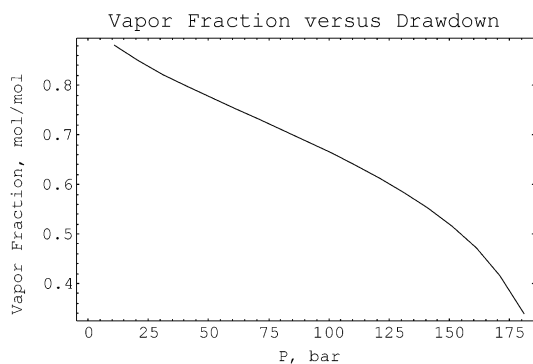


Fig. 7. Scenario 1: pressure drawdown. Vapor fraction of a mixture as a function of pressure (at constant temperature).

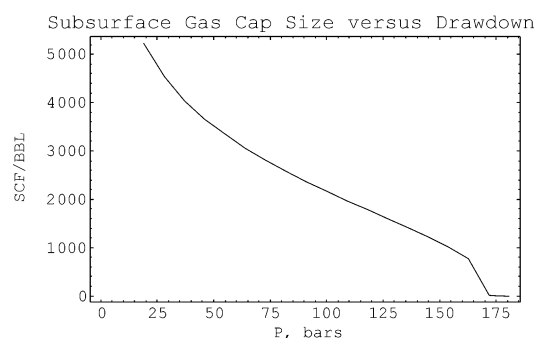


Fig. 8. Change in gas cap size as a function of reservoir pressure (at a constant temperature).

gas cap size. However, the increase in the amount of material (moles or grams) in the gas cap increases less quickly, and so is better indicated by vapor fraction.

In scenario two (the production scenario), a pressure drawdown is simulated by removing liquid from the mixture (i.e. production of the oil leg). In general, the actual coupling between amount of material removed and pressure reduction is a complex function of hydrodynamic regime and reservoir geometry beyond the scope of this monograph. To avoid unnecessary and confusing complexity, we arbitrarily assign a ‘removal ratio’ (amount of mixture removed/pressure drop) of 0.01 bar<sup>-1</sup>: removal of 1% of the mixture by mole decreases pressure by one bar. Of course, other conditions will correspond to other ratios.

The two scenarios described here have different resultant states. By producing the liquid fraction (oil leg) of a reservoir, we would expect the fraction of the mixture in the vapor phase to approach unity as all liquid is removed. Indeed it does, as shown by Fig. 9. In this figure, we see that the produced reservoir always has a larger amount of material in the vapor phase than the drawdown mixture. The produced reservoir ‘taps out’—i.e. becomes one-phase vapor—at approximately 80 bar. In contrast, pressure draw-down decreases but does not eliminate the liquid leg.

Modeling chemical changes from fractionation can help to predict the differences between the two scenarios. Traditional applications of equations of state rely on pseudo-components to account for complex hydrocarbon composition. However, the use of pseudo-components does not foreclose the use of real components in the mixture. In particular, compounds of interest to the geochemist, such as biomarkers or geochemical fingerprinting compounds, can be included in the models. For example, consider the mixture used before, where we include several ‘fingerprinting’ compounds. If one carefully includes compounds in the simulation whose affinity for either liquid or vapor phases is roughly similar

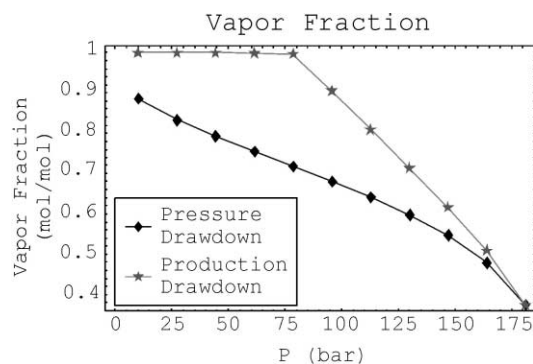


Fig. 9. Vapor fraction for each scenario (pressure drawdown without production and production-induced pressure drawdown).

at the pressures and temperatures of the reservoir, these compounds can act as ‘fingerprints’ for the processes that the reservoir is experiencing. This idea is not new—fingerprinting reservoirs is an important tool of the reservoir geochemist—but using equations of state to model processes allows the geochemist to better interpret the fingerprints.

A reservoir geochemist might be interested in how a pressure-drawdown in a reservoir affects the fractionation of the fingerprint compounds into the gas cap. Here the question would be twofold: (1) are the current fingerprinting compounds appropriate to compare a produced reservoir with a virgin reservoir and (2) can equations of state be used for screening more appropriate and less volatile fingerprinting compounds.

As an example of this, consider the two scenarios specified above: a mixture in a reservoir, composed of material as specified in Table 1. We will divide several of the pseudo-components into constituent compounds, which we will use for fingerprinting. Though generally this is done using actual GC data, we are only concerned with developing the tool, and so we will use ‘typical’ values for the components (derived from averaging about 30 Gulf-Coast oils). The fingerprint compounds are listed below, in relative mole fractions (i.e. mole fractions such that the sum of all compounds at each carbon number is one):

The fingerprinting compounds defined in Table 2 are used by replacing the pseudo-component with the appropriate amounts of the fingerprinting compounds. For example, according to Table 1 0.704% of the mixture consists of undifferentiated C10 compounds. By introducing the fingerprinting compounds into the model, we replace this C10 pseudo-component with 22.5% naphthalene and 77.5% *n*-decane. A good test for the legitimacy of this action is to test whether this addition changes either the density or phase behavior of the mixture. A quick calculation shows this is not so.

Table 2  
Fingerprinting compounds

Carbon Number	Species	Relative mole fraction
7	Toluene	0.301
7	Methylcyclohexane	0.317
7	<i>n</i> -Heptane	0.212
7	2-Methylhexane	0.143
7	2,2-Dimethylpentane	0.027
8	Ethylbenzene	0.204
8	<i>n</i> -Octane	0.541
8	<i>trans</i> -1,2-Dimethylcyclohexane	0.073
8	2,3-Dimethylhexane	0.056
8	2-Methylheptane	0.126
10	Naphthalene	0.225
10	<i>n</i> -Decane	0.775

Details of the calculation are found in the web section of this work.

Once the fingerprinting compounds have been added to the test mixture, the two scenarios—iso-compositional depressurization and pressure decline with simultaneous liquid removal—can be compared. The changes in composition are shown in Fig. 10. In this figure, the lines represent the mole fractions within the liquid (oil) phase of the C8 fingerprinting compounds in a Radar plot format. At each test pressure, the composition of the liquid is estimated, the concentrations of the fingerprinting compounds extracted, and plotted. Since a decrease in pressure tends to concentrate C8 compounds in the liquid phase, concentrations from lower pressures are found outside those from higher pressures. The two scenarios are superimposed to show the effects of the different scenarios directly. Fig. 10 shows that, with increasing liquid production, the fingerprint of the liquid phase (shown in gray) drifts from simple pressure-induced fractionation (shown in black). This is most clearly shown in the *n*-octane/ethylbenzene ratio, and in the ethylbenzene/2-methyl heptane ratio. Here, the gray lines cut the black lines, indicating that the ratios for these compounds are affected by the difference in the scenarios. Other ratios, such as *t*-1,2 dimethylcyclohexane versus 2,3-dimethylhexane, do not show much change. Here the gray and black lines remain parallel at all pressures.

This can be seen even more clearly by looking at the relationship between heavier compounds. Fig. 11 shows the ratio between naphthalene and *n*-decane in the two scenarios. Shown here are the ratios in both the liquid and vapor phases for the depressurization versus production scenario. Since *n*-decane is more volatile than naphthalene, the mole fraction ratio of naphthalene to *n*-decane is smaller in the vapor phase than in the liquid phase. Hence, producing the liquid phase tends to selectively remove naphthalene, bringing the mole fraction ratios closer together. This can be seen particularly

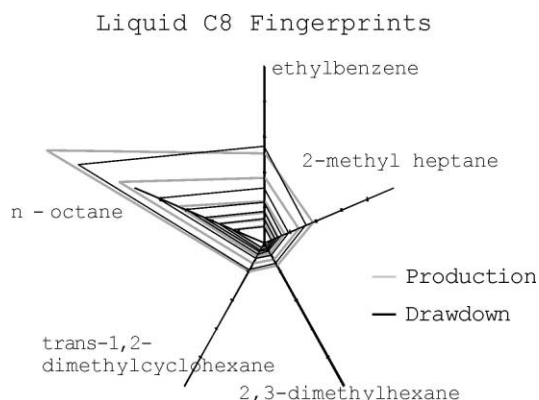


Fig. 10. Comparing fingerprints for a production scenario (in gray) and a pressure decline (in black).

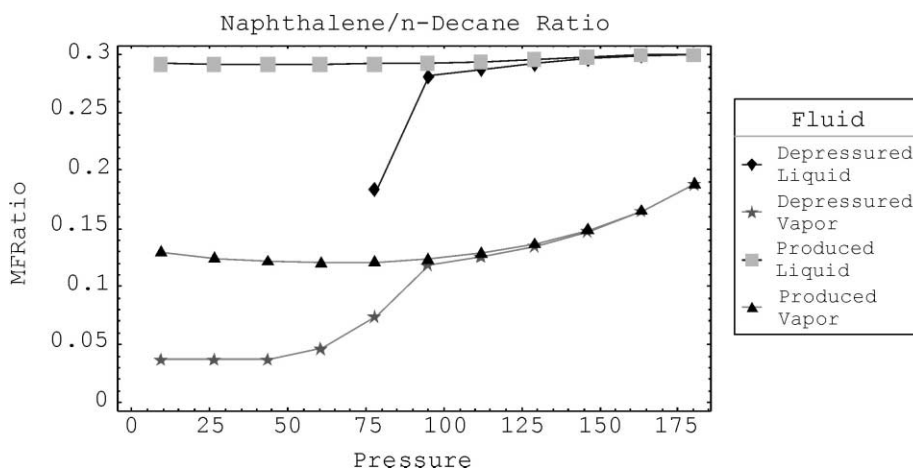


Fig. 11. Ratio of naphthalene and *n*-decane (C10) in the two scenarios.

in the produced liquid ratio naphthalene/*n*-decane ratio, which drops from 0.3 at the initial reservoir pressure to about 0.28 at 100 bars pressure. The largest difference between the two scenarios occurs between 100 and 80 bar, where the amount of material in the liquid is approaching zero. Note that at approximately 80 bar pressure, the produced scenario fluid becomes a one-phase vapor (all liquid has been produced), and so further production, and further fractionation, is no longer possible.

This example shows that, by simulating different scenarios using the appropriately complex mixture in equations of state, the processes that effect reservoir composition can be distinguished. This can have immediate bottom-line consequences in such issues as production allocation, reservoir delineation, and indirect estimates of reservoir conditions. A careful use of equation of state calculations can limit, for example, the number of actual pressure measurements to which a reservoir need be subjected. Since pressure measurements represent time the reservoir is not producing, equation of state modeling can directly impact the bottom line profitability of a reservoir.

### 6.3. Exploration issues

#### 6.3.1. Fractionation

The frontier of usage for equations of state involves using them, in conjunction with a basin model, to predict the properties and composition of complex mixtures from source rock to reservoir. This involves predicting the results of repeated mixing and separations. The value of such predictions is that:

- a better knowledge of the fluid flow environment is ascertained,
- quality and quantity risk management issues can be addressed, and

- Samples of deeper fluids might be embedded within known fluids.

In the simulations presented here, one-dimensional finite difference models are developed to highlight the role of equations of state in fluid property estimation.

The first exploration example involves simulation of evaporative fractionation. Evaporative fractionation (Thompson, 1987) involves vapor-phase fractionation where a fluid is mixed with/invaded by a gas flow, and then re-equilibrates at a lower pressure. The more gas added to the original mixture, the greater the fractionation. When a subsurface fluid is subjected to evaporative fractionation, the event produces two single-phase fluids (known as ‘daughter’ fluids); a fractionated liquid and an evaporative condensate. If the liquid and vapor phases of such an even are separated, each carries the mark of having been through the evaporative fractionation scheme.<sup>4</sup> Liquids tend to lose their light (e.g. gasoline range) ends to the vapor phase, but be saturated in methane. Condensates tend to have a high load of dissolved heavy ends (C12+) compared to thermal condensates. We can use equations of state to predict the composition of these fluids after fractionation in several reasonable situations. This work does not attempt to fully explore evaporative fractionation; instead, we simply show several examples to demonstrate the utility of equations of state to understanding a complex fluid interaction problem.

In order to simulate evaporative fractionation, we will use the test mixture defined in Table 1 modified as in the above example with fingerprinting compounds. We

<sup>4</sup> Note that, without this physical segregation of the two phases, the mixture is not fractionated, since all material original material is still present. The composition of each phase has changed, however.

simulate the invasion of the original mixture by some amount of methane. After invasion, the two phases migrate to a shallower depth then physically separate. There are two variables of interest in the problem: depth of separation, and amount of methane mixed into the liquid. Evaporative fractionation is simulated using an equation of state by taking the mixture from Table 1 and creating a series of new “daughter” mixtures by adding different amounts of gas to  $x$  changes in composition due to evaporative fractionation.

The addition of methane can change oil to volatile oil or even condensate, as shown by Fig. 12. The figure shows the vapor fraction of the each daughter mixture as a function of depth and fraction methane. The effects to the original mixture’s phase behavior of adding methane are as follows. As more methane is added, the daughter mixture’s bubble depth (the depth at which the vapor fraction goes to zero) increases; that is, the mixture requires higher pressures to dissolve all the methane present in the system. With larger amounts of added methane the daughter mixture becomes supercritical, and eventually an evaporative condensate. The dew depth (depth at which the vapor fraction drops below 1) actually starts to decrease when extreme amounts of methane are added to the mixture, since the large excesses of methane become under saturated with respect to the heavy oil components present.

Thompson (1987) predicts, based on a number of experiments and a large number of field observations, that evaporative fractionates should show distinctive compositional trends in species of similar carbon number but different structure (e.g. toluene/*n*-heptane ratio).

A closer examination of the compositions predicted by the flash calculations should yield the distinctive compositional trends created by evaporative fractionation. For example, Fig. 13 shows the cross plot of two ratios of species found in the liquid phase: *n*-hexane/benzene ( $H/B$ ) versus *n*-decane/naphthalene ( $D/N$ ). A hallmark of the fractionation scenarios described above (either pressure- or production-fractionation) is that fractionation was most intense between species of differing carbon number. For example, in Fig. 11, the naphthalene/*n*-decane ratio changes very slightly over most of the range, until the mixture approaches its dew point at the quite low pressure of 100 bar. By adding methane, this change can be exaggerated, as shown in Fig. 13.

Fig. 13 shows the change in the ratio between *n*-hexane and benzene ( $H/B$  ratio) cross-plotted with the change in the ratio between *n*-decane and naphthalene ( $D/N$  ratio) as a function of amount of gas and mixture depth. Each line in the figure shows the evolution of a mixture, defined by how much additional methane has been added to the original mixture, with curve, though the absolute magnitude of changes increases with increasing amounts of gas. For each figure, the curve describes a tilted ‘u’ shape: at shallowest depths, the  $D/N$  ratio reaches a local maximum. With increasing depth, both the  $D/N$  ratio and the  $H/B$  ratio decrease. At some depth, unique for each mixture, both the  $D/N$  and the  $H/B$  ratio reach a global minimum. At increasing depths beyond this critical depth, both ratios increase monotonically. At shallower conditions, the  $H/B$  ratio changes more rapidly than the  $D/N$  ratio, while at deeper conditions, the opposite is true.

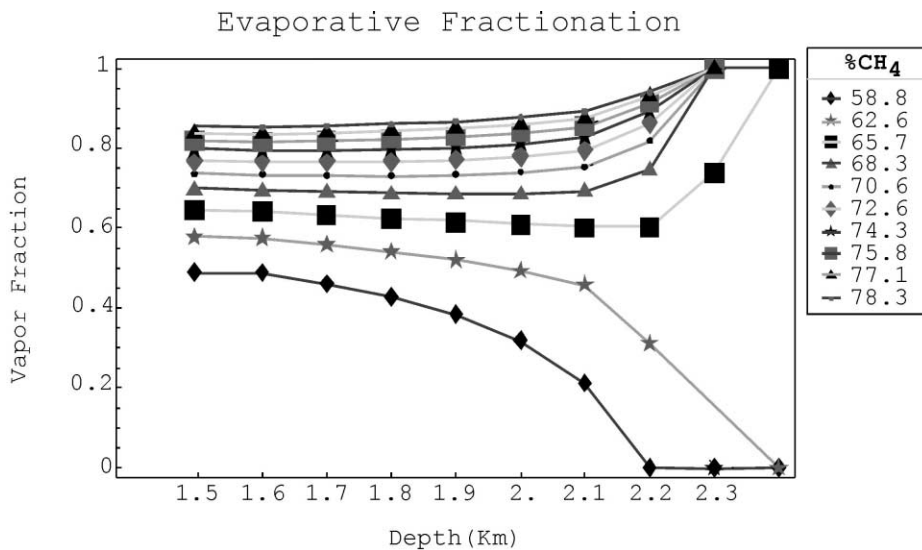


Fig. 12. Evaporative fractionation vapor fraction. Shown here is the amount of material (fraction, by mole) in the vapor phase as a function of depth for each mixture.

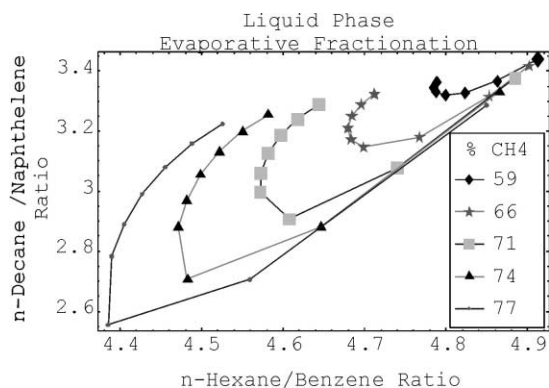


Fig. 13. Ratio of species in the liquid phase after evaporative fractionation. As the amount of methane in the mixture increases, the amount of fractionation (change in ratios with depth) also increases.

In order to interpret this diagram, one must realize:

- (1) Heavier compounds are less soluble in the vapor phase than lighter compounds from the same chemical class.
- (2) As depth increases, the solubility differences identified in (1) tend to increase in importance.
- (3) The relative solubilities of aromatic and aliphatic compounds of similar molecular weight in the vapor phase changes with  $(P, T)$  conditions and with mixture composition.
- (4) The more vapor-like the mixture (i.e. the more methane in the mixture), the greater the solubility differences between aromatic and aliphatic compounds.
- (5) The solubility of aromatic compounds in the vapor phase in these examples seems to be less sensitive to changes in pressure-temperature than aliphatic compounds. As the amount of gas in the mixture goes up, the sensitivity declines even more.
- (6) The closer a two-phase fluid is to the phase boundary (i.e. vapor fraction near 0 or 1), the more fractionation occurs.

The effects of evaporative fractionation are also imprinted in the composition of the vapor phase (the evaporative condensate). Fig. 14 shows the changes in the  $D/N$  and the  $H/B$  ratio in the vapor phase as a function of the amount of methane added to the mixture and of the  $(P, T)$  conditions of the mixture. Fig. 14 shows that both the  $D/N$  and the  $H/B$  ratios decrease linearly with depth, until all mixtures take on a single value for each ratio (the value found in the original mixture). The convergence towards this single value simply reflects the phase state of the mixture; each mixture is two-phase at the lowest  $(P, T)$  conditions, and

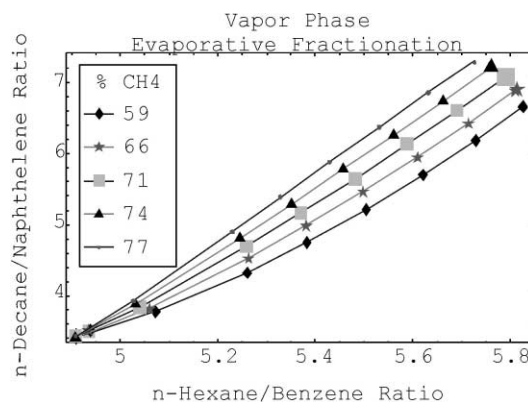


Fig. 14. Ratio of species in the vapor phase after evaporative fractionation. As the amount of methane in the mixture increases, the amount of fractionation (change in ratios with depth) tends to remain fairly constant.

each becomes one-phase by the highest  $(P, T)$  conditions (see Fig. 12). At  $(P, T)$  conditions between the two extremes, each mixture has unique values for the two ratios. In general, larger amounts of methane added to a mixture tend to decrease the  $H/B$  ratio, and increase the  $D/N$  ratio, while increasing depth tends to decrease both ratios.

The behavior of the vapor phase in evaporative fractionation for this mixture is much more regular than the behavior of the liquid phase. The ratios discussed here are skewed with respect to the values of the ratios within the original mixture, following a regular, linear pattern. Solubility differences tend to be erased in the vapor phase as the vapor fraction of a mixture approaches a phase boundary (0 or 1). The residual, liquid, phase tends to emphasize these differences, although the fraction of each species in the residual phase goes monotonically to zero as that phase is dissolved into the vapor phase with increasing  $(P, T)$ .

### 6.3.2. Gas washing

As a final example, we model gas washing, as defined by this author (Meulbroek, 1997). Gas washing describes a scenario where a fluid is repeatedly 'washed' (i.e. mixed with) a migrating high maturity gas condensate stream. The vapor phase continues to migrate after washing, removing volatile components from the liquid. The mixing is assumed to occur under equilibrium conditions, and is thus amenable to equation of state simulation. The effect of gas washing is to strip the original fluid of its most volatile components, and to change the original fluid's composition over time to reflect relative solubility differences in components. Gas washing is documented in several areas of the US gulf coast (Meulbroek et al., 1999), and is thought to occur worldwide, including offshore Taiwan, the North Sea, and offshore Mahakam Delta, Indonesia. The effects of

gas washing are strongly dependent on the ( $P$ ,  $T$ ) conditions under which the washing takes place, and the amount of gas with which the fluid interacts. A common scenario for gas washing is an oil, temporarily trapped at the top of overpressure, washed by gas leaking through the top of overpressure.

Simulating gas washing is a good example with which to explore the utility of equations of state in exploration. Unlike any of the previous examples, gas washing describes an open-system fractionation in which composition tends to change over time. It thus becomes much more difficult to model than e.g. evaporative fractionation, since the effects on composition of gas washing are so dependant on initial and boundary conditions. Since previous results based on similar models have been presented in the literature, this example will simply compare gas washing to the other fractionation phenomena, and demonstrate how modeling the phenomena using equations of state can clarify the differences in the effects of each phenomena. By understanding the effects of different phenomena, regions where the phenomena are important can be identified, and exploration strategies can be tailored to minimize risk and maximize potential.

Gas washing is simulated using a simple finite difference scheme. The mixture defined above in Table 1, modified using the fingerprinting compounds, is equilibrated at a series of ( $P$ ,  $T$ ) conditions designed to lie along a depth trajectory. At each of these ( $P$ ,  $T$ ) conditions the mixture undergoes the following procedure:

- to each mixture, some volume of gas is mixed and flashed to achieve equilibrium,
- from the vapor phase an amount of equilibrated vapor (that is, gas with some amount of dissolved

liquid) is removed. The amount of material removed is equal in volume to the volume of methane added,

- the mixture is re-flashed, and the process repeated.

The volumes used at each step are small enough to avoid convergence effects, determined by trial and error. There are two independent variables of interest in the scenarios: the depth at which the washing takes place and the amount of gas involved in the washing. Note that this simple one-dimensional model can hide a lot of complexity. To expand this simulation beyond one phase, the volume of gas added at each step should be a function of flow rates and flow path structure.

The results of the simulation should be understood by looking at the changes in mixture composition, and in the composition of each phase, as a function of time/amount of flow. Unlike the previous scenarios, the total mixture (liquid + vapor) tends to change over time, since methane is added and a complex vapor mixture is removed at each time step. Fig. 15 shows the change in the two ratios used to explore evaporative fractionation ( $n$ -hexane/benzene,  $H/B$  and  $n$ -decane/naphthalene,  $D/N$ ) as a function of depth of washing and amount of flow. The mixtures at each depth start with the same ratios, but diverge over time in response to depth-specific solubility differences. This figure shows.

- (1) Greater depths of washing lead to greater alteration.
- (2) A larger or longer flow leads to greater alteration.
- (3) The two effects are additive; more gas has more of an effect at greater depths.

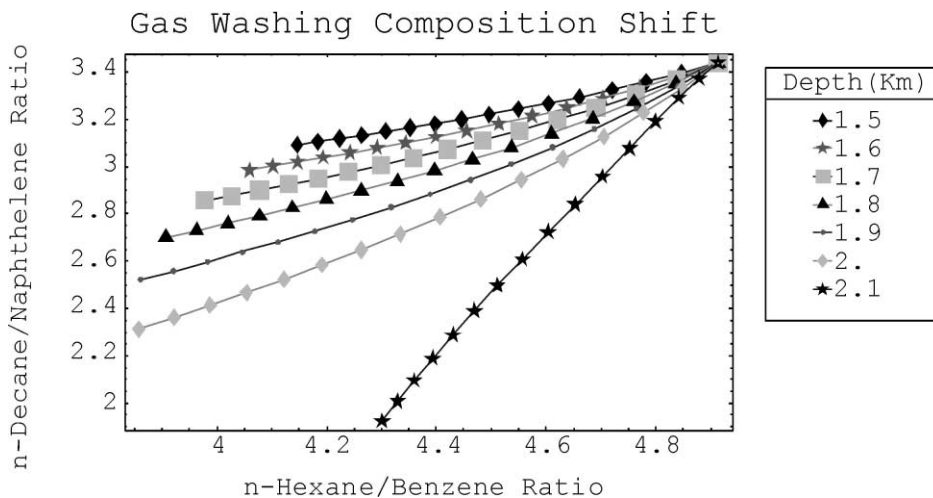


Fig. 15. Compositional shift due to gas washing.



Adding gas to a mixture tends to drive the phase behavior of that mixture towards a condensate, but the effect is depth-dependant. Fig. 16 shows the effect on the vapor fraction of gas washing as a function of amount of gas at different depths. Each curve represents the results of a gas washing simulation at a specific depth. At shallow conditions, the effects of washing on vapor fraction are minimal; the vapor fraction increases slightly, but not significantly. At these conditions, the vapor fraction can actually *decline* over time with increasing washing. This counter-intuitive result is easily explained: as the gas washing removes the most soluble components of the mixture, these components are not available to go into the vapor phase, and the entire residual mixture becomes more insoluble in methane. As the depth of washing increases, more and more components become soluble in the vapor, and the amount of residual decreases over time as it is washed away. Finally, at some depth (2.2 km, in this simulation), the entire mixture is soluble in the vapor phase, and is removed quickly by gas washing. Note that this

simulation is unrealistic in the sense that no solid or high molecular weight components (such as asphaltenes) are present in the test mixtures. These compounds would presumably fractionate much less strongly than the compounds used in the simulation, leaving a residual liquid phase that would be more resistant to washing.

The results of washing defined above are confirmed in Fig. 17, which shows the change in the liquid phase of the two ratios defined above by gas washing at different depths. Each line in this figure represents an independent simulation. All mixtures start at the same set of ratios in the upper right corner of the figure, but quickly diverge with continual washing. Both ratios fall with increasing washing, as the more aliphatic compound in each ratio is removed at a faster rate than the aromatic compound by the gas stream. Both ratios fall more quickly per unit added gas with increasing depth, as the solubility differences between the ratio compounds are increased by increased (*P*, *T*) conditions. Although with greater depth, more of all four components are removed, proportionately more of the aliphatic compounds are removed as depth increases. As shown in this diagram, the deeper the washing, the greater the fractionation in the liquid phase.

The composition of the vapor phase is a little more complex, and can be understood in reference to evaporative fractionation. The early stages of gas washing are analogous to evaporative fractionation, in that a body of fluid is mixed with a high maturity fluid, and the phases physically separated. Hence, we would expect the initial ratio to increase with depth, as occurs for evaporative fractionation in Fig. 14. In fact, the initial values for the ratios (circled in Fig. 18) do increase with

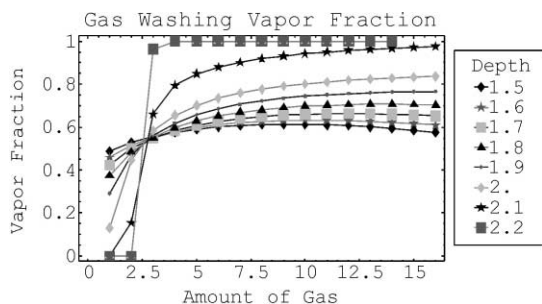


Fig. 16. Vapor fraction of gas-washed mixture.

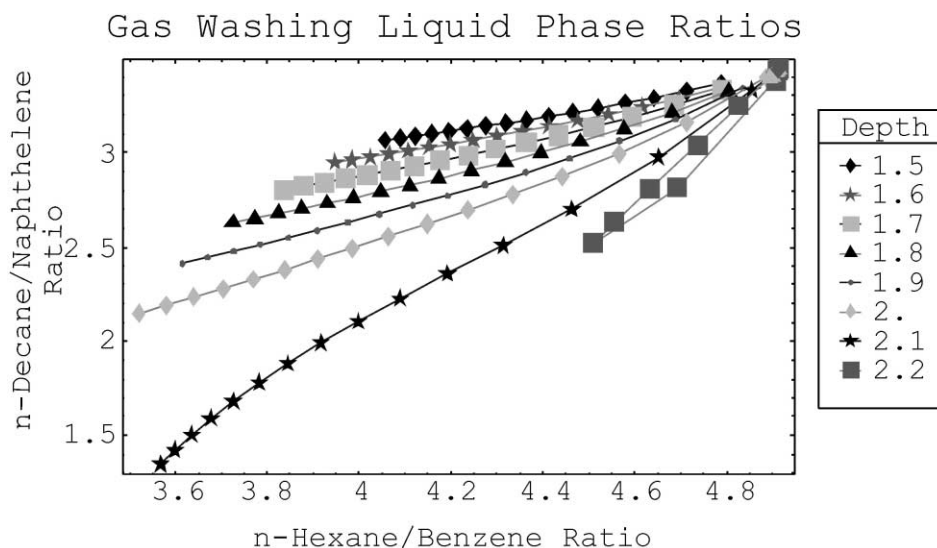


Fig. 17. Gas washing liquid phase ratios.

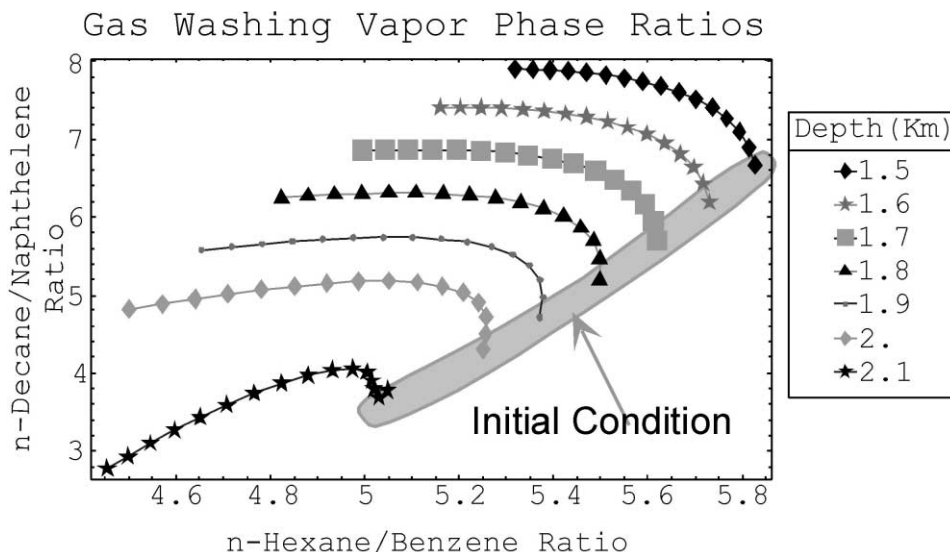


Fig. 18. Vapor phase ratios. The starting ratios (ratios present in the first batch of gas) are circled.

depth. In later stages of the simulation after some gas has washed the mixture, the washing alters the composition of the mixture, resulting in less aliphatic compounds being available to be washed (they have already been removed). Since the ratios in each mixture get lower as each simulation progresses (see Fig. 15), the ratios in the vapor phase become progressively lower. Comparing the ratios between liquid and vapor phase shows, however, that the ratios are always higher in the vapor phase than the liquid phase. The trend towards declining ratios with increased washing is first noticeable in the  $(H/B)$  ratio since these compounds are more soluble in gas than the  $(D/N)$  ratio compounds.

Gas washing is a complex scenario that is difficult to understand without the use of numeric modeling based on equations of state. The modeling allows the user to examine multiple scenarios quickly, and predict trends in composition. In a natural setting, when unusual compositions are seen, these compositions can be compared to predictions made using the numeric models, with a better understanding of the natural system resulting.

## 7. Conclusion

Equations of state have been used by the chemical and chemical engineering communities for the past several hundred years. Early definers of equations of state are Boyle, Charles, and Avagadro. Fluid Phase Equilibria models are somewhat younger, being defined by the mathematization of thermodynamics under Gibbs, Hemholtz, et al., circa 1880. When the two types of

models are combined, a powerful predictive tool is revealed.

Equations of state have been used in the petroleum industry since at least the 1940s. Early models include that by Redlich and Kwong, and by Benedict, Webb and Rubin. Traditional use of the equation of state has been to interpolate predictions of reservoir fluid bulk properties, such as GOR and density. This original use did not require an extensive knowledge of the composition of the fluid. A mixture might be characterized, e.g. by a distillation run, where the abundances of boiling point fractions determined the properties of the mixture. More recently, a pseudo-distillation might identify the 7 or 8 most common species, with the rest of the mixture lumped together into 1 or more-pseudo-components of unknown composition.

With the advent of more sophisticated chemical models and more powerful computers, mixtures of greater complexity can be examined using equations of state. The utility of these models in non-traditional roles such as reservoir management, production allocation, and exploration is evident. This work presented examples of using equations of state to understand compositional shifts in both the reservoir and the migration conduit. In the reservoir, equations of state can make predictions that can be used to distinguish depressurization fractionation from production fractionation, and thus help delineate reservoir compartments. In the migration conduit, equations of state can explore the effects of multiphase migration on oil composition. The hope is to then be able to recognize distinguishing characteristics of migration processes within the oil, leading to a better understanding of subsurface processes.

Two migration phenomena are examined: evaporative fractionation and gas washing. The two phenomena are distinguishable by the compositional marks they leave in fractionated fluids. evaporative fractionation, as has been reported elsewhere, yields gases enriched in aliphatic compounds, and liquids enriched in aromatic compounds. Using equations of state, the conditions under which an evaporative fractionation occurs can be deduced from the composition of the residual phases. Gas washing tends to produce condensates that are enriched in aromatic compounds. The liquid phase tends to be heavy, heavily enriched in aromatics, and have a high amount of solution gas.

It is hoped that, by utilizing equations of state, organic geochemists can leverage the large amount of information available to them to understand both anthropomorphic and non-anthropomorphic hydrocarbon alteration. Alteration can have profound influence on the abundance and quality of available resources. Organic geochemists can measure the quantity present in a fluid of an almost unlimited number of compounds. Each of these compounds can act as an indicator of different sub-surface processes. Using equations of state with traditional organic geochemistry, a much more thorough understanding of the subsurface can result.

### Acknowledgements

I wish to offer special thanks to Dr. Gordon MacLeod for comments and review, Dr. Lawrence Cathles and Dr. William Goddard III for support and comments, the ACS for initial support, participants in the “ACS EOS In Exploration” Special Session, and the Gas Research Institute for funding.

### Appendix A. Redlich–Kwong equation of state

For pure species,  $b$  is defined as follows:

$$b = \frac{0.08664RT_c}{P_c}, \quad (5)$$

where  $T_c$  is the fluid’s critical temperature, and  $P_c$  is the fluid’s critical pressure. The attraction parameter,  $a$ , is a function of temperature and the critical properties of the fluid as follows:

$$a = \frac{0.42748R^2T_c^{2.5}}{P_cT^{1/2}}, \quad (6)$$

where  $T$  is the system absolute temperature.

The Redlich–Kwong equation of state is applied to fluid mixtures by defining mixing rules for parameters  $a$

and  $b$ . The mixing function given by Redlich and Kwong for  $b$  is a linear average of  $b$  values of the individual components in the fluid mixture:

$$b = \sum_i x_i b_i. \quad (7)$$

In the above equation,  $x_i$  is the mole fraction of the  $i$ th species in the mixture, and  $b_i$  is the incompressible volume of the  $i$ th pure species, calculated by Eq. (5).

The Redlich–Kwong  $a$  parameter is a geometric average of  $a$  values of individual components in the fluid mixture:

$$a = \sum_i \sum_j x_i x_j k_{ij} \sqrt{a_i a_j}. \quad (8)$$

In the above equation,  $a_i$  and  $a_j$  are the pure component attraction parameters, and  $k_{ij}$  is an empirical interaction parameter, determined from experimental data. More information on  $k_{ij}$  can be found below. The Redlich–Kwong equation of state proved to be acceptable for mixtures of chemically similar species, and remained popular from its inception (in 1946) until the early 1970’s.

#### A.1. Soave mixing rules

Soave (1972) remedied this shortcoming by modifying Eq. (8) by replacing  $a$  with  $\alpha$ , which is defined as follows:

$$\alpha_i = a_i \left[ 1 + \kappa_i \left( 1 - \sqrt{T_{r,i}} \right) \right]^2 \quad (9)$$

In the above,  $a_i$  is the pure-species attraction parameter for species  $i$ , calculated by Eq. (6), and  $\kappa_i$  is a quadratic function of  $\omega_i$ , the accentric factor.  $T_{r,i}$  is the  $i$ th component’s reduced temperature, and is defined as follows:

$$T_{r,i} = \frac{T}{T_{c,i}}. \quad (10)$$

The right-hand term (in brackets) of Eq. (9) was added by Soave to better model the temperature dependence of the attraction parameter for molecules of different accentricities. Since the temperature dependence is stronger for non-spherical molecules, the  $\kappa_i$  term is defined by a quadratic polynomial in  $\omega_i$ , as follows:

$$\kappa_i = 0.37464 + 1.54225\omega_i - 0.26992\omega_i^2. \quad (11)$$

The range of accentric factors for  $n$ -alkanes between  $C_1$  and  $C_{50}$  is 0 to 1.5;  $\kappa_i$  monotonically increases over that range, from 0.5 to 2.0.

## A.2. Calculating fugacity

A thermodynamic system reaches the minimum Gibbs Free Energy when all phases are stable, and the fugacity of each component in the system is constant across all phases. In this context, stability means that the creation of a new phase of any composition raises system Gibbs free energy (Michelsen, 1982a,b). To calculate the composition of each phase requires the fugacity of each component in each phase. The fugacity of a species can be thought of as the partial pressure of that species, adjusted by the species' non-ideal behavior. Fugacity can be calculated by the following equation (Prausnitz et al., 1986):

$$\ln[\phi_i] = \frac{1}{RT} \int_{\infty}^V \frac{RT}{V} - \frac{dP}{dn_i} dV - \ln \left[ \frac{Pv}{RT} \right], \quad (12)$$

where  $\phi$  in the above equation is the fugacity coefficient, defined by

$$\phi_i = \frac{f_i}{x_i P}. \quad (13)$$

In the above,  $R$  is the universal gas constant,  $T$  is the system temperature,  $P$  is the system pressure,  $v$  is the system molar volume,  $x_i$  is the mole fraction of the  $i$ th component, and  $f_i$  is the fugacity of  $i$ th component, and  $V$  is the system total volume. Note that the following relationship holds:

$$v = \frac{V}{N}, \quad (14)$$

where  $N$  is the total number of moles of material in the system. At the limit of zero pressure (hence, infinite volume), the fugacity of a component in a mixture is equal to its partial pressure, and the fugacity coefficient [as defined by Eq. (12)] is unity. Eq. (4) is completely general, and can be applied to any species in any phase.

In order to solve for fugacity, an expression for the derivative of pressure with respect to composition must be found. Since an equation of state relates pressure and composition, the derivative of pressure with respect to composition can be found (Szarawara, and Gawdzik, 1989), and then integrated to calculate the fugacity coefficient. The following equation results from applying an RKS-type equation of state to Eq. (4):

$$\ln[\phi_i] = -\ln \left[ \frac{RT(v-b)}{Pv^2} \right] + \frac{b+B'[x_i]}{v-b} - \frac{a(b+B'[x_i])}{bRT(v+b)} - \frac{\ln \left[ \frac{v+b}{v} \right] (bA'[x_i] + a(b-B'[x_i]))}{b^2 RT}, \quad (15)$$

where

$$B'[n_i] = \sum_{j=1}^m (b_i + b_j)x_j - 2b, \quad (16)$$

and

$$A'[n_i] = 2 \sum_{j=1}^m \sqrt{\alpha_i \alpha_j} k_{ij} x_j - 2a, \quad (17)$$

$b$  is defined from Eq. (7),  $a$  is defined from Eq. (8), and all other symbols are defined as before.

## Appendix B. The flash model

A fluid phase equilibria model finds the number of phases and the distribution of species among these phases, that minimizes Gibbs Free Energy. The following describes a variant of fluid phase equilibria model that calculates the equilibrium phase conditions of a mixture as a function of pressure, temperature, and composition. This type of model is often referred to as a flash model. The algorithm is based loosely on previous work (Ahmed, 1989; Edminister and Lee, 1988). A flash model can in principle consider a mixture that separates into more than two phases (Enick et al., 1986; Bünz, Dohrn, and Prausnitz, 1991), though the current implementation is restricted to a two-phase model.

The following definitions will be used in the derivation. The equilibrium constant,  $K$ , is defined as follows:

$$K_i = \frac{y_i}{x_i}, \quad (18)$$

where  $y_i$  is the mole fraction of the  $i$ th species in the vapor phase, and  $x_i$  is the mole fraction of the  $i$ th species in the liquid phase. The fugacity coefficient  $\phi_i$  of the  $i$ th species is defined as

$$\phi_i = \frac{f_i}{x_i P}, \quad (19)$$

where  $f_i$  is the fugacity of the  $i$ th species. At the limit of infinite volume (zero pressure),  $\phi$  is unity. A flash model is based on the assumption that the fugacities of all species are identical in both phases. Mathematically:

$$f_i^L = f_i^V \quad \forall i \quad (20)$$

Combining Eqs. (17), (18) and (19) results in the following relationship:

$$K_i = \frac{\phi_{i,L}}{\phi_{i,V}} \quad (21)$$

A second necessary assumption for a flash model is conservation of mass for each species in the system. Hence, each species partitions between the liquid and vapor phases, as follows:

$$M_F z_i = M_V y_i + M_L x_i \quad \forall i, \quad (22)$$

where  $M_F$  is the total moles of material in the system,  $M_V$  is the total moles of material in the vapor phase,  $M_L$  is the total moles of material in the liquid phase, and  $z_i$  is the mole fraction of the  $i$ th species in the system.

The total mass is also conserved for the system, and is divided between the two phases as follows:

$$M_F = M_V + M_L \quad (23)$$

Finally, the mole fractions of each species sum to unity, as follows:

$$\sum_{i=1}^m z_i = \sum_{i=1}^m x_i = \sum_{i=1}^m y_i = 1 \quad (24)$$

Combining Eqs. (18) and (21) yields the following relationships for  $x_i$  and  $y_i$ :

$$x_i = \frac{z_i}{S + K_i - SK_i} \quad (25)$$

and

$$y_i = \frac{K_i z_i}{S + K_i - SK_i} \quad (26)$$

In the above equation,  $S$  is defined as the liquid fraction of the system. This can be written as:

$$S = M_L / M_F \quad (27)$$

By definition,  $S$  must fall between 0 and 1, inclusively. The difference of Eqs. (24) and (25) can be substituted into Eq. (26) and summed over  $i$  to result in:

$$\sum_i \frac{(K_i - 1)z_i}{(1 - S)K_i + S} = 0. \quad (28)$$

Eq. (27) relates the equilibrium constant of each species,  $K_i$ , and the liquid fraction  $S$  in one equation that does not depend explicitly on the mole fraction of material in each phase. This equation is solved in the following iterative procedure (Rijkers and Heidemann, 1986):

- (1) Start with an estimation for  $K_i$ .
- (2) Solve Eq. (27) for  $S$  using a Newton–Raphsen convergence procedure.

(3) Given  $S$  and  $K$  from step 2, use Eqs. (24) and (25) to obtain  $x_i$  and  $y_i$ .

(4) Substitute these values into Eq. (14) to obtain the fugacity coefficients  $\phi_{i,L}$  and  $\phi_{i,V}$  for each species in the mixture.

(5) Use the fugacity coefficients obtained from step 4 in Eq. (20) to update the guess for  $K_i$ .

(6) Repeat Steps 2–5 until the changes in the values of  $K_i$  for each iteration fall below some arbitrary convergence criteria. A typical convergence criteria is:

$$\sum_i \Delta K_i < 10^{-10}. \quad (29)$$

## References

- Aasberg-Petersen, K., Stenby, E., 1991. Prediction of thermodynamic properties of oil and gas condensate mixtures. *Industrial & Engineering Chemical Research* 30, 248–254.
- Ahmed, T., 1989. *Hydrocarbon Phase Behavior*, Contributions in Petroleum Geology and Engineering, Vol. 7. Gulf, Houston.
- Altgelt, K.H., Boduszynski, M.M., 1996. *Composition and Analysis of Heavy Petroleum Fractions*. Marcel Dekker, New York.
- Behar, E., Simonet, R., Rauzy, E., 1985. A new non-cubic equation of state. *Fluid Phase Equilibria* 21, 237–255.
- Braun, Robert L., Burnham, Alan K., 1990. Mathematical model of oil generation, degradation, and expulsion. *Energy and Fuels* 4, 132–146.
- Bünz, A.P., Dohrn, R., Prausnitz, J.M., 1991. Three-phase flash calculations for multicomponent systems. *Computers in Chemical Engineering* 15, 47–51.
- Chou, G.F., Prausnitz, J.M., 1989. A phenomenological correction to an equation of state for the critical region. *AIChE Journal* 35, 1487–1496.
- Dahl, S., Michelsen, M.L., 1991. High-pressure vapor-liquid equilibrium with a uniaxial-based equation of state. *AIChE Journal* 36, 1829–1836.
- di Primio, R., Dieckmann, V., Mills, N., 1998. PVT and phase behaviour analysis in petroleum exploration. *Organic Geochemistry* 29, 207–222.
- di Primio, R., 2002. Unraveling secondary migration effects through the regional evaluation of PVT data. A case study from Quadrant 25, NOCS. *Organic Geochemistry* 33, this issue.
- Dzou, L.I., Hughes, W.B., 1993. Geochemistry of oils and condensates, K field, offshore Taiwan: a case study in migration fractionation. *Organic Geochemistry* 20, 437–462.
- Edmister, W.C., Lee, B.I., 1988. *Applied Hydrocarbon Thermodynamics*. Gulf, Houston.
- England, W.A., 1990. The organic geochemistry of petroleum reservoirs. *Organic Geochemistry* 16, 415–425.
- Enick, R.M., Hlder, G.D., Grenko, J.A., Brainard, A.J., 1986. Four-phase flash equilibrium calculations for multicomponent systems containing water. In: *Equations of State: Theories and Applications*, ACS Symposium Series 300, pp. 494–518.

- Fredenslund, Aa., Gmehling, J., Rasmussen, P., 1977. Vapor-Liquid Equilibrium Using UNIFAC. Elsevier, New York.
- Holderbaum, T., Gmehling, J., 1991. PSRK: a group contribution equation of state based on UNIFAC. *Fluid Phase Equilibria* 70, 251–265.
- Kvenvolden, K.E., Claypool, G.E., 1980. Origin of gasoline-range hydrocarbons and their migration by solution in carbon dioxide in Norton Basin, Alaska. *AAPG Bulletin* 64, 1078–1106.
- Larter, S., Mills, N., 1991. Phase-controlled molecular fractionations in migrating petroleum charges. In: England and Fleet (Eds.) *Petroleum Migration*. Geological Society Special Publication No. 59, 137–147.
- Lielmezs, J., Mak, P.C.N., 1992. Thermodynamic properties of unsaturated vapour and liquid states from a cubic equation of state: saturated and subcritical regions. *Thermochimica Acta* 196, 415–435.
- Lin, C-T, Daubert, T.E., 1978. Prediction of the fugacity coefficients of nonpolar hydrocarbon systems from equations of state. *Industrial Engineering Chemical Process Design Development* 17, 544–549.
- Mathias, Paul M., 1983. A versatile phase equilibrium equation of state. *Industrial Engineering Chemical Process Design Development* 22, 385–391.
- McAuliffe, C.D., 1979. Oil and gas migration-chemical and physical constraints. *AAPG Bulletin* 63, 761–778.
- Meulbroek, P., Taylor, P., Lynch, M., 1999. Phase fractionation and migration history of fluids from vermilion blocks 14 and 39, Gulf of Mexico, USA. Presented to the 1999 European Association of Organic Geochemistry meeting, 5–8 September, 1999, Istanbul, Turkey.
- Meulbroek, P., 1997. Hydrocarbon Phase Fractionation in Sedimentary Basins. PhD thesis, Cornell University, Ithaca, New York.
- Michelsen, M.L., 1982. The isothermal flash problem: part 1: stability. *Fluid Phase Equilibria* 9, 1–19.
- Michelsen, M.L., 1982. The isothermal flash problem: part 2: phase-split calculation. *Fluid Phase Equilibria* 9, 21–40.
- Michelsen, Michael L., 1990. A method for incorporating excess gibbs energy models into equations of state. *Fluid Phase Equilibria* 60, 47–58.
- Pendersen K. S., Fredenslund Aa., Thomassen P., 1989. Properties of oils and natural gases, Contributions in Petroleum Geology and Engineering, vol. 5. Gulf, Houston.
- Pendersen, K.S., Thomassen, P., Fredenslund, A., 1984. Thermodynamics of petroleum mixtures containing heavy hydrocarbons. 3. Efficient flash calculation procedures using the SRK equation of state. *Industrial Engineering Chemical Process Design Development* 23, 948–9544.
- Prausnitz, J.M., Lichtenthaler, R.N., de Azevedo, E.G., 1986. *Molecular thermodynamics of fluid-phase equilibria*, second ed. Prentice-Hall, Upper Saddle River New Jersey.
- Price, Leigh C., 1976. Aqueous solubility of petroleum as applied to its origin and primary migration. *AAPG Bulletin* 60, 213–244.
- Redlich, O., Kwong, J.N.S., 1949. *Chemical Review* 44, 233.
- Reid, R., Prausnitz, J.M., Sherwood, T., 1985. *The Properties of Gases and Liquids*, Fourth ed. McGraw-Hill, New York.
- Rijkers, P.W., Heidemann, R.A., 1986. Convergence behavior of single-stage flash calculations. *Equations of State: Theories and Applications*, ACS Symposium Series 300, pp. 477–493.
- Shibata, Steven K., Sandler, Stanley I., 1989. Critical evaluation of equation of state mixing rules for the prediction of high-pressure phase equilibria. *Industrial and Engineering Chemical Research* 28, 1893–1898.
- Shock, E.L., Helgeson, H.C., 1990. Calculation of the thermodynamic and transport properties of aqueous species at high pressures and temperatures: standard partial molal properties of organic species. *Geochimica et Cosmochimica Acta* 54, 915–945.
- Silverman, S.R., 1963. Migration and segregation of oil and gas. *AAPG Bulletin* 47, 2075–2076.
- Silverman, S.R., Plumley, W.J., 1963. Separation-Migration, An Hypothesis for Explaining Compositional Differences Among Related Petroleum. Research Report No. 809, California Research Corporation, La Habra, CA.
- Soave, G., 1972. Equilibrium constants from a modified Relich-Kwong equation of state. *Chemical Engineering Science* 27, 1197–1203.
- Sokolov, V.A., Zhuse, T.P., Vassoyevich, N.B., Antonov, P. L., Grigoriyev, G. G., Kozlov, V. P., 1963. Migration Processes of Gas and Oil, Their Intensity and Directionality. Sixth WPC, Frankfurt.
- Sylta, Oyvind, 1991. Modelling of secondary migration and entrapment of a multicomponent hydrocarbon mixture using equation of state and ray-tracing modeling techniques. In: England and Fleet (Ed.), *Petroleum Migration*, Geological Society Special Publication, No. 59, pp. 111–122.
- Szarawara, J., Gawdzik, A., 1989. Method of calculation of fugacity coefficient from cubic equation of state. *Chemical Engineering Science* 44, 1489–1494.
- Thompson, K.F.M., 1987. Fractionated aromatic petroleum and the generation of gas-condensates. *Organic Geochemistry* 11, 573–590.
- Tsonopoulos, C., Heidman, J.L., 1986. High-pressure vapor-liquid equilibria with cubic equations of state. *Fluid Phase Equilibria* 29, 391–414.
- van der Waals, J.D., 1873. Over de Continuïteit van den Gas- en Vloeistoftoestand (On the continuity of the gas and liquid state).
- Vandenbroucke, M., Durand, B., 1983. Detecting migration phenomena in a geological series by means of C1–C35 hydrocarbon amounts and distributions. *Advances In Organic Geochemistry* 1981, 147–155.
- Vidal, J., Lermite, C., 1979. A group contribution equation of state for polar and non-polar compounds. *Fluid Phase Equilibria* 72, 111–130.
- Wang, L.S., Gmehling, J., 1999. Improvement of the SRK equation of state for representing volumetric properties of petroleum fluids using Dortmund Data Bank. *Chemical Engineering Science* 54, 3885–3892.
- Wendebourg, J., 2000. Modeling multi-component petroleum fluid migration in sedimentary basins. *Journal of Geochemical Exploration* 69, 651–656.
- Zhang, Quanxing, Zhang, Qiming, 1991. Evidence of primary migration of condensate by molecular solution in aqueous phase in Yacheng field, offshore south China. *Journal of Southeast Asia Earth Sciences* 5, 101–106.